Higgs- and *Z*-boson Production with a Jet Veto

Andrea Banfi,[1] Pier Francesco Monni,[2] Gavin P. Salam,[3,4,5] and Giulia Zanderighi[6]

[1]*Albert-Ludwigs-Universität Freiburg, Physikalisches Institut, D-79104 Freiburg, Germany*
[2]*Institut für Theoretische Physik, Universität Zürich, CH-8057 Zürich, Switzerland*
[3]*CERN, PH-TH, CH-1211 Geneva 23, Switzerland*
[4]*Department of Physics, Princeton University, Princeton, New Jersey 08544, USA*
[5]*LPTHE, CNRS UMR 7589, UPMC University of Paris 6, 75252 Paris cedex 05, France*
[6]*Rudolf Peierls Centre for Theoretical Physics, 1 Keble Road, University of Oxford, Oxford OX13NP, United Kingdom*

We derive first next-to-next-to-leading logarithmic resummations for jet-veto efficiencies in Higgs and
Z-boson production at hadron colliders. Matching with next-to-next-to-leading order results allows us to
provide a range of phenomenological predictions for the LHC, including cross-section results, detailed
uncertainty estimates, and comparisons to current widely used tools.

In searches for new physics at hadron colliders such as the Tevatron and CERN's Large Hadron Collider (LHC), in order to select signal events and reduce backgrounds, events are often classified according to the number of hadronic jets (collimated bunches of energetic hadrons) in the final state. A classic example is the search for Higgs production via gluon fusion with a subsequent decay to W^+W^- [1,2]. A severe background comes from $t\bar{t}$ production, whose decay products also include a W^+W^- pair. However, this background can be separated from the signal because its W^+W^- pair usually comes together with hard jets, since in each top decay the *W* is accompanied by an energetic (*b*) quark.

Relative to classifications based on objects such as leptons (used, e.g., to identify the *W* decays), one of the difficulties of hadronic jets is that they may originate not just from the decay of a heavy particle, but also as quantum chromodynamic radiation. This is the case in our example, where the incoming gluons that fuse to produce the Higgs boson quite often radiate additional partons. Consequently, while vetoing the presence of jets eliminates much of the $t\bar{t}$ background, it also removes some fraction of signal events. To fully interpret the search results, including measuring Higgs couplings, it is crucial to be able to predict the fraction of the signal that survives the jet veto, which depends, for example, on the transverse momentum threshold $p_{t,\text{veto}}$ used to identify vetoed jets.

One way to evaluate jet-veto efficiencies is to use a fixed-order perturbative expansion in the strong coupling α_s, notably to next-next-to-leading order (NNLO), as in the Higgs-boson production calculations of Refs. [3–5]. Such calculations, however, become unreliable for $p_{t,\text{veto}} \ll M$, with *M* the boson mass, since large terms $\alpha_s^n L^{2n}$ appear [$L = \ln(M/p_{t,\text{veto}})$] in the cross section to all orders in the coupling constant. These enhanced classes of terms can, however, be resummed to all orders in the coupling, often involving a functional form $\exp(Lg_1(\alpha_s L) + g_2(\alpha_s L) + \alpha_s g_3(\alpha_s L)/\pi + \ldots)$.

There exist next-to-next-to-leading logarithmic (NNLL) resummations, involving the $g_n(\alpha_s L)$ functions up to and including g_3, for a number of quantities that are more inclusive than a jet veto: e.g., a Higgs or vector-boson transverse momentum [6–9], the beam thrust [10], and related observables [11,12]. To obtain estimates for jet vetoes, some of these calculations have been compared to or used to reweight [10,13–16] parton-shower predictions [17,18] matched to NLO results [19,20]. However, with reweighting, neither the NNLO nor NNLL accuracy of the original calculation carries through to the jet-veto prediction.

Recently there has been progress towards NNLL calculations of the jet-veto efficiency itself. Full NLL results and some NNLL ingredients for Higgs and vector-boson production were provided in Ref. [21]. Reference [22] used these and other ingredients in the soft-collinear effective theory framework to consider resummation for the Higgs-boson case beyond NLL accuracy. In this Letter we show how to use the results of Ref. [21] together with those from boson p_t resummations [6–9] to obtain full NNLL accuracy. We also examine the phenomenological impact of our results, including a matching to NNLO predictions. Given the ubiquity of jet cuts in hadron-collider analyses, the understanding gained from our analysis has a potentially wide range of applications.

The core of boson transverse-momentum (p_t^B) resummations lies in the fact that soft, collinear emissions at disparate rapidities are effectively emitted independently. Summing over all independent emissions, one obtains the differential boson p_t cross section

$$\frac{d\Sigma^{(B)}}{d^2\vec{p}_t^B} = \sigma_0 \int \frac{d^2\vec{b}}{4\pi^2} e^{-i\vec{b}\cdot\vec{p}_t^B} \sum_n \frac{1}{n!} \prod_{i=1}^n \int [dk_i] M^2(k_i)(e^{i\vec{b}\cdot\vec{k}_{ti}} - 1),$$

(1)

where σ_0 is the leading-order total cross section, $[dk_i]M^2(k_i)$ is the phase space and matrix element for

emitting a soft, collinear gluon of momentum k_i, while the exponential factors and b integral encode in a factorized form the constraint relating the boson p_t and those of individual emissions $\delta^2(\vec{p}_t^B - \sum_{i=1}^n \vec{k}_{ti})$ [23]. The -1 term in the round brackets arises because, by unitarity, virtual corrections come with a weight opposite to that of real emissions, but do not contribute to the p_t^B sum.

To relate Eq. (1) to a cross section with a jet veto, let us first make two simplifying assumptions: that the independent-emission picture is exact and that a jet algorithm clusters each emission into a separate jet. The resummation for the cross section for the highest jet p_t to be below some threshold $p_{t,\text{veto}}$, considering jets at all rapidities, is then equivalent to requiring all emissions to be below that threshold:

$$\Sigma^{(J)}(p_{t,\text{veto}})$$
$$= \sigma_0 \sum_{n=0}^{\infty} \frac{1}{n!} \prod_{i=1}^{n} \int [dk_i] M^2(k_i)(\Theta(p_{t,\text{veto}} - k_{ti}) - 1)$$
$$= \sigma_0 \exp\left[-\int [dk] M^2(k) \Theta(k_t - p_{t,\text{veto}}) \right], \quad (2)$$

with the same universal matrix element $M^2(k)$ entering Eqs. (1) and (2).

Equation (2) is clearly an oversimplification. Firstly, even within the independent emission picture, two emissions close in rapidity y and azimuth ϕ can be clustered together into a single jet. Let us introduce a function $J(k_1, k_2)$ that is 1 if k_1 and k_2 are clustered together and 0 otherwise. Concentrating on the 2-emission contribution to Eq. (2), one sees that clustering leads to a correction given by the difference between the veto with and without clustering:

$$\mathcal{F}^{\text{clust}} \sigma_0 = \frac{\sigma_0}{2!} \int [dk_1][dk_2] M^2(k_1) M^2(k_2)$$
$$\times J(k_1, k_2)(\Theta(p_{t,\text{veto}} - k_{t,12})$$
$$- \Theta(p_{t,\text{veto}} - k_{t1})\Theta(p_{t,\text{veto}} - k_{t2})), \quad (3)$$

where $k_{12} = k_1 + k_2$ (throughout, we assume standard E-scheme recombination, which adds 4-vectors). This contribution has a logarithmic structure $\alpha_s^2 L$, i.e., NNLL, with each emission leading to a power of α_s, while the L factor comes from the integral over allowed rapidities [$|y| \lesssim \ln(M/p_{t,\text{veto}})$].

For more than two emissions, two situations are possible: (i) three or more emissions are close in rapidity, giving extra powers of α_s without extra log enhancements (N³LL and beyond); (ii) any number of extra emissions are far in rapidity, each giving a factor $\alpha_s L$, i.e., also NNLL. The latter contribution is simple because, independently of whether the two nearby emissions clustered, those that are far away must still have $p_{ti} < p_{t,\text{veto}}$. Thus the full *clustering* correction to the independent-emission picture is a multiplicative factor $(1 + \mathcal{F}^{\text{clust}})$, as first derived in detail in the appendix of Ref. [21] using results from Ref. [24].

For the generalized-k_t jet-algorithm family [25–29], with a jet radius parameter R, we have $J(k_1, k_2) = \Theta(R^2 - (y_1 - y_2)^2 - (\phi_1 - \phi_2)^2)$. At NNLL accuracy, Eq. (3) evaluates to $\mathcal{F}^{\text{clust}} = 4\alpha_s^2(p_{t,\text{veto}})CLf^{\text{clust}}(R)/\pi^2$ with (see Ref. [21])

$$f^{\text{clust}}(R) = \left(-\frac{\pi^2 R^2}{12} + \frac{R^4}{16}\right)C, \quad (4)$$

for $R < \pi$; C is $C_F = \frac{4}{3}$ or $C_A = 3$, respectively, for incoming quarks (e.g., $q\bar{q} \rightarrow Z$) or incoming gluons (e.g., $gg \rightarrow H$).

Next, we address the issue that gluons are not all emitted independently. This is accounted for in Eq. (1) because, to order α_s^2, the $M^2(k)$ quantity that appears there should be understood as an effective matrix element

$$[dk]M^2(k) = [dk](M_1^2(k) + M_{1\text{-loop}}^2(k)) + \int d^2\vec{k}_t [dk_a]$$
$$\times [dk_b] M_{\text{correl}}^2(k_a, k_b)\delta^2(\vec{k}_{t,ab} - \vec{k}_t) \quad (5)$$

where $M_1^2(k)$ is the pure $\mathcal{O}(\alpha_s)$ matrix element, $M_{\text{correl}}^2(k_a, k_b)$ the correlated part of the matrix element for the emission of two soft-collinear gluons or a quark-antiquark pair, including relevant symmetry factors, and $M_{1\text{-loop}}^2$ the corresponding part of the α_s^2 1-loop matrix element. The separation into correlated and independent emissions is well defined because of the different color factors that accompany them in the generic case [30–33]. The δ function in Eq. (5) extracts two-parton configurations with the same total p_t as the 1-gluon configurations.

For a jet veto, part of the result from the effective matrix element carries through: when two correlated emissions are clustered into a single jet, it is their sum, $\vec{k}_{t,ab}$, that determines the jet transverse momentum. Therefore the same effective matrix element can be used in Eq. (2), as long as one includes an additional correction to account for configurations where the two emissions are clustered in separate jets:

$$\mathcal{F}^{\text{correl}} \sigma_0 = \sigma_0 \int [dk_a][dk_b] M_{\text{correl}}^2(k_a, k_b)$$
$$\times [1 - J(k_a, k_b)](\Theta(p_{t,\text{veto}} - k_{ta})\Theta(p_{t,\text{veto}} - k_{tb})$$
$$- \Theta(p_{t,\text{veto}} - k_{t,ab})). \quad (6)$$

at NNLL accuracy, $\mathcal{F}^{\text{correl}} = 4\alpha_s^2(p_{t,\text{veto}})CLf^{\text{correl}}(R)/\pi^2$ with (see Ref. [21])

$$f^{\text{correl}}(R) = \left(\frac{(-131 + 12\pi^2 + 132\ln 2)C_A}{72}\right.$$
$$\left. + \frac{(23 - 24\ln 2)n_f}{72}\right)\ln\frac{1}{R} + 0.61C_A$$
$$- 0.015n_f + \mathcal{O}(R^2), \quad (7)$$

for generalized-k_t algorithms, in the limit of small R. Reference [21] includes a numerical result for all $R < 3.5$ and analytical terms up to R^6, used in the rest of this Letter. It did not, however, make the relation with the boson p_t resummation.

All remaining contributions to a NNLL resummation, such as the 3-loop cusp anomalous dimension or a multiplicative $C_1\alpha_s$ term are either purely virtual, so independent of the precise observable, or involve at most a single real emission, so can be taken from the boson p_t resummations [6–9]. (For generic processes, subtleties can arise with spin-correlation effects [34]. These are simpler for jet vetoes, which do not correlate distinct collinear regions). Thus the full NNLL resummed cross section for the jet veto is given by

$$\Sigma_{\mathrm{NNLL}}^{(J)}(p_{t,\mathrm{veto}}) = \sum_{i,j}\int dx_1 dx_2 |\mathcal{M}_B|^2 \delta(x_1 x_2 s - M^2)\Bigg[f_i(x_1, e^{-L}\mu_F)f_j(x_2, e^{-L}\mu_F)\left(1 + \frac{\alpha_s}{2\pi}\mathcal{H}^{(1)}\right)$$
$$+ \frac{\alpha_s}{2\pi}\frac{1}{1 - 2\alpha_s\beta_0 L}\sum_k \int_{x_1}^1 \frac{dz}{z}\left(C_{ki}^{(1)}(z)f_i\left(\frac{x_1}{z}, e^{-L}\mu_F\right)f_j(x_2, e^{-L}\mu_F)\right)$$
$$+ \{(x_1, i)\leftrightarrow(x_2, j)\}\Bigg)\Bigg](1 + \mathcal{F}^{\mathrm{clust}} + \mathcal{F}^{\mathrm{correl}})e^{Lg_1(\alpha_s L)+g_2(\alpha_s L)+(\alpha_s/\pi)g_3(\alpha_s L)}, \tag{8}$$

where the coefficient functions $\mathcal{H}^{(1)}$ and $C_{ki}^{(1)}$, and resummation functions g_1, g_2, and g_3 are as derived for the boson p_t resummation [6,7,9] (reproduced for completeness in the Supplemental Material [35], together with further discussion on the connection to boson p_t resummation). The results are expressed in terms of $L = \ln(Q/p_{t,\mathrm{veto}})$, $\alpha_s \equiv \alpha_s(\mu_R)$; the resummation, renormalization, and factorization scales Q, μ_R, and μ_F are to be chosen of order of M.

A form similar to Eq. (8) was derived independently in Ref. [22] for Higgs production, also using ingredients from Ref. [21]. It differs, however, at NNLL in that the combination of $f^{\mathrm{clust}} + f^{\mathrm{correl}}$ is accompanied by an extra $-\zeta_3 C_A$. Reference [22] had used a NNLL analysis of the $R \to \infty$ limit to relate jet and boson-p_t resummations. A subtlety of this limit is that one must then account for a N³LL $\alpha_s^2 R$ term, which for $R \gtrsim \ln M/p_t$ is promoted to an additional NNLL $\alpha_s^2 \ln M/p_t$ contribution [35].

One check of Eq. (8) is to expand it in powers of α_s, $\Sigma_{\mathrm{NNLL}}^{(J)}(p_t) = \alpha_s^2 \sum_{n=0}^\infty \Sigma_{\mathrm{NNLL},n}^{(J)}(p_t)$, and compare $d\Sigma_{\mathrm{NNLL},2}^{(J)}(p_t)/d\ln p_t$ to the NLO Higgs + 1 jet prediction [36–38] from the Monte Carlo for FeMtobarn processes (MCFM) [39], $d\Sigma_2^{(J)}(p_t)/d\ln p_t$. NNLL resummation implies control of terms $\alpha_s^2 L^3 \ldots \alpha_s^2$ (constant terms) in this quantity and so the difference between MCFM and the second order expansion of the resummation should vanish for large L. This is what we find within reasonable precision. The precision of the test can be increased if one considers the $\mathcal{O}(\alpha_s^2)$ difference between the jet and boson-p_t resummations, which has fewer logarithms and so is numerically easier to determine in MCFM. It is predicted to be

$$\frac{d\Sigma_{\mathrm{NNLL},2}^{(J)}(p_t)}{d\ln p_t} - \frac{d\Sigma_{\mathrm{NNLL},2}^{(B)}(p_t)}{d\ln p_t}$$
$$= -\frac{4C\alpha_s^2\sigma_0}{\pi^2}(f^{\mathrm{clust}}(R) + f^{\mathrm{correl}}(R) + \zeta_3 C). \tag{9}$$

This is compared to MCFM's LO H + 2-jet result in the upper panel of Fig. 1. There is excellent agreement at small p_t, for each of three R values. The result of Ref. [22] (BN, only for $R = 0.5$) is also shown for comparison.

The above test can be extended one order further by examining the order $\alpha_s^3\sigma_0$ difference between the jet and boson p_t differential distributions. The comparison between our predictions and MCFM H + 2-jet NLO results [40,41] is given in Fig. 1 (lower panel), for each of the three R values (we use here a different center-of-mass energy and Higgs mass compared to the LO calculation to improve
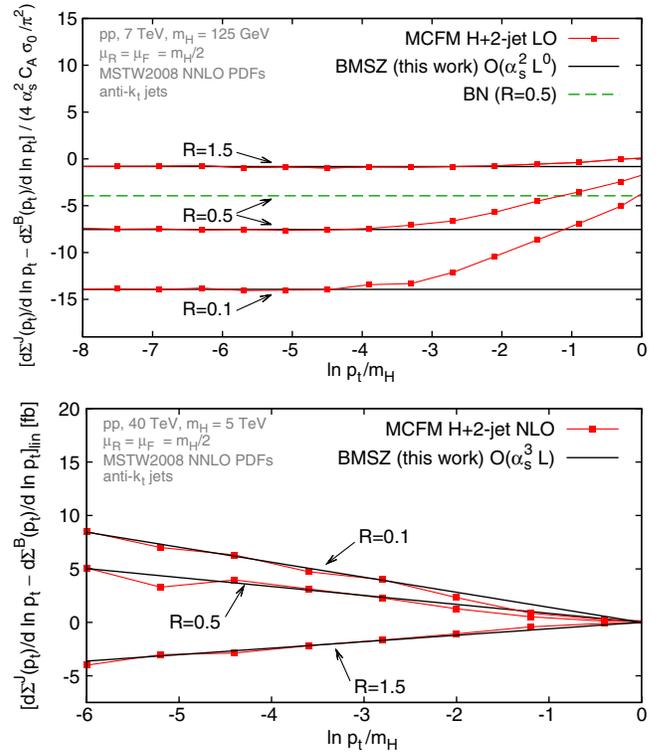

FIG. 1 (color online). Upper panel: second order difference between jet and Higgs-boson $\ln p_t$ differential distributions, showing the coefficient of $4\alpha_s^2 C_A\sigma_0/\pi^2$ as determined with MCFM and predicted in Eq. (9), for three R values. We also show the prediction from Ref. [22] (BN). Lower panel: differences at $\mathcal{O}(\alpha_s^3\sigma_0)$ between jet and boson $\ln p_t$ differential distributions, with the expected $\alpha_s^3\sigma_0 L^2$ term subtracted (denoted by a subscript lin), showing the MCFM H + 2-jet NLO result compared to our NNLL prediction for the $\alpha_s^3\sigma_0 L$ term.
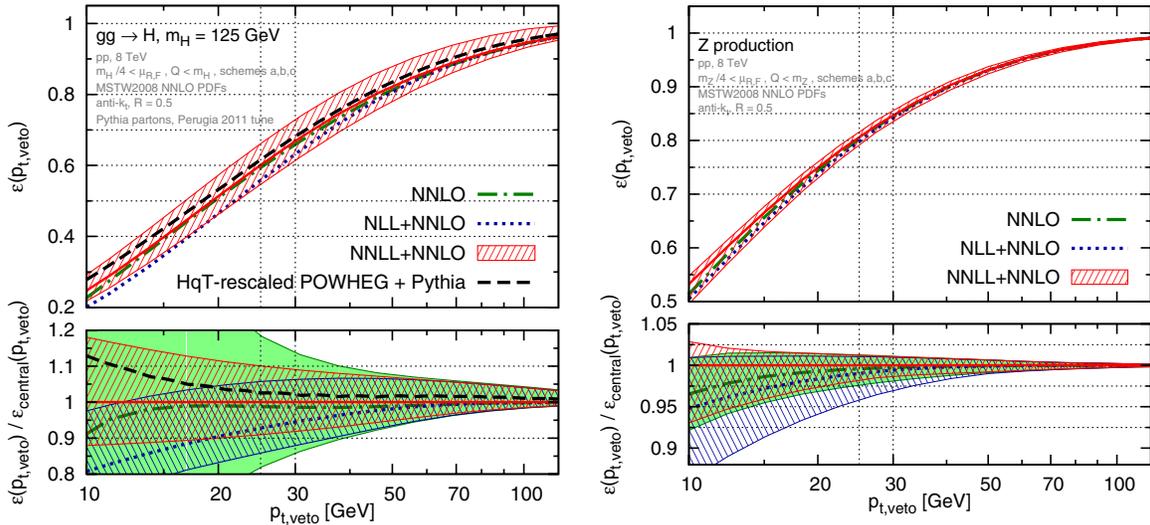
FIG. 2 (color online).   Comparison of NNLO (dot-dashed line, solid band), NLL + NNLO (dotted line, downwards-right oblique band), and NNLL + NNLO (solid line, upwards-right oblique band) results for jet-veto efficiencies for Higgs (left) and Z-boson (right) production at the 8 TeV LHC. The Higgs plot includes the result from a POWHEG (revision 1683) [20,55] plus Pythia (6.426) [17,56] simulation (dashed line) in which the Higgs-boson p_t distribution was reweighted to match the NNLL + NNLO prediction from HqT 2.0 [7] as in Ref. [21]. The lower panels show results normalized to the central NNLL + NNLO efficiencies.

the convergence of MCFM). To facilitate visual interpretation of the results, the expected $\alpha_s^3 \sigma_0 L^2$ term has been subtracted. The residual $\alpha_s^3 \sigma_0 L$ term is clearly visible in the MCFM results and, within the fluctuations, coincides well with our predictions, providing a good degree of corroborating evidence for the correctness of our results beyond order $\alpha_s^2 \sigma_0$.

To illustrate the phenomenological implications of our work, we examine the jet-veto efficiency $\epsilon(p_t) \equiv \Sigma^{(J)}(p_t)/\sigma_{\text{tot}}$, where σ_{tot} is the total cross section, known up to NNLO [42–47]. We combine (*match*) the resummation with fixed-order predictions, available from fully differential NNLO boson-production calculations [4,5,48,49] or NLO boson + jet calculations [36,50] implemented in MCFM [51]. We use three matching schemes, denoted *a*, *b*, and *c*, straightforward extensions [35] of those used at NLL in Ref. [21].

Our central predictions have $\mu_R = \mu_F = Q = M/2$ and use scheme *a* matching, with MSTW2008NNLO PDFs [52]. We use the anti-k_t [29] jet-algorithm with $R = 0.5$, as implemented in FASTJET [53]. For the Higgs case we use the large m_{top} approximation and ignore $b\bar{b}$ fusion and b's in the $gg \to H$ loops (corrections beyond this approximation have a relevant impact [16,54]). To determine uncertainties we vary μ_R and μ_F by a factor of 2 in either direction, requiring $1/2 \leq \mu_R/\mu_F \leq 2$. Maintaining central $\mu_{R,F}$ values, we also vary Q by a factor of 2 and change to matching schemes *b* and *c*. Our final uncertainty band is the envelope of these variations (cf. Ref. [21]). In the fixed-order results, the band is just the envelope of $\mu_{R,F}$ variations.

The results for the jet-veto efficiency in Higgs and Z-boson production are shown in Fig. 2 for 8 TeV LHC

collisions. Compared to pure NNLO results, the central value is slightly higher and for Higgs production, the uncertainties reduced, especially for lower $p_{t,\text{veto}}$ values. Compared to NNLO + NLL results [21], the central values are higher, sometimes close to the edge of the NNLO + NLL bands; since the NNLO + NLL results used the same approach for estimating the uncertainties, this suggests that the approach is not unduly conservative. In the Higgs case, the NNLO + NNLL uncertainty band is not particularly smaller than the NNLO + NLL one. This should not be a surprise, since Ref. [21] highlighted the existence of possible substantial corrections beyond NNLL and beyond NNLO accuracy. For the Higgs case, we also show a prediction from POWHEG [20,55] interfaced to Pythia 6.4 [17] at parton level (Perugia 2011 shower tune [56]), reweighted to describe the NNLL + NNLO Higgs-boson p_t distribution from HqT (v2.0) [7], as used by the LHC experiments. Though reweighting fails to provide NNLO or NNLL accuracy for the jet veto, for $p_{t,\text{veto}}$ scales of practical relevance, the result agrees well with our central prediction. It is, however, harder to reliably estimate uncertainties in reweighting approaches than in direct calculations.

Finally, we provide central results and uncertainties for the jet-veto efficiencies and 0-jet cross sections (in pb) with cuts (in GeV) like those used by ATLAS and CMS, and also for a larger R value:

R	$p_{t,\text{veto}}$	$\epsilon^{(7\ \text{TeV})}$	$\sigma^{(7\ \text{TeV})}_{0\text{-jet}}$	$\epsilon^{(8\ \text{TeV})}$	$\sigma^{(8\ \text{TeV})}_{0\text{-jet}}$
0.4	25	$0.63^{+0.07}_{-0.05}$	$9.6^{+1.3}_{-1.1}$	$0.61^{+0.07}_{-0.06}$	$12.0^{+1.6}_{-1.4}$
0.5	30	$0.68^{+0.06}_{-0.05}$	$10.4^{+1.2}_{-1.1}$	$0.67^{+0.06}_{-0.05}$	$13.0^{+1.5}_{-1.5}$
1.0	30	$0.64^{+0.03}_{-0.05}$	$9.8^{+0.8}_{-1.1}$	$0.63^{+0.04}_{-0.05}$	$12.2^{+1.1}_{-1.4}$

Interestingly, the $R = 1$ results have reduced upper uncertainties, due perhaps to the smaller value of the NNLL $f(R)$ correction [a large $f(R)$ introduces significant Q-scale dependence]. The above results are without a rapidity cut on the jets; the rapidity cuts used by ATLAS and CMS lead only to small, $<1\%$, differences [21].

For the 0-jet cross sections above, we used total cross sections at 7 and 8 TeV of $15.3^{+1.1}_{-1.2}$ and $19.5^{+1.4}_{-1.5}$ pb, respectively [57,58] (based on results including Refs. [43–47]) and took their scale uncertainties to be uncorrelated with those of the efficiencies. Symmetrizing uncertainties, we find correlation coefficients between the 0-jet and ≥ 1-jet cross sections of $-0.43\,(-0.50)$ for $R = 0.4\,(R = 0.5)$, using the covariance matrix in Ref. [35].

The code to perform the resummations and matchings shown here is publicly available [59].

Note added.—As our manuscript was being finalised, Ref. [60] appeared. It claims issues in NNLL resummations of jet vetoes; however, it does not address the all-order derivation of the NNLL R-dependent terms in Ref. [21]. Its claim is further challenged by the α_s^3 numerical check in Fig. 1.

[1] S. Chatrchyan *et al.* (CMS Collaboration), Phys. Lett. B **710**, 91 (2012).

[2] G. Aad *et al.* (ATLAS Collaboration), Phys. Lett. B, **716**, 62 (2012).

[3] S. Catani, D. de Florian, and M. Grazzini, J. High Energy Phys. 01 (2002) 015.

[4] C. Anastasiou, K. Melnikov, and F. Petriello, Nucl. Phys. **B724**, 197 (2005).

[5] S. Catani and M. Grazzini, Phys. Rev. Lett. **98**, 222002 (2007); M. Grazzini, J. High Energy Phys. 02 (2008) 043.

[6] G. Bozzi, S. Catani, D. de Florian, and M. Grazzini, Phys. Lett. B **564**, 65 (2003).

[7] G. Bozzi, S. Catani, D. de Florian, and M. Grazzini, Nucl. Phys. **B737**, 73 (2006).

[8] G. Bozzi, S. Catani, G. Ferrera, D. de Florian, and M. Grazzini, Phys. Lett. B **696**, 207 (2011).

[9] T. Becher and M. Neubert, Eur. Phys. J. C **71**, 1665 (2011).

[10] C. F. Berger, C. Marcantonini, I. W. Stewart, F. J. Tackmann, and W. J. Waalewijn, J. High Energy Phys. 04 (2011) 092.

[11] A. Banfi, M. Dasgupta, and S. Marzani, Phys. Lett. B **701**, 75 (2011).

[12] A. Banfi, M. Dasgupta, S. Marzani, and L. Tomlinson, Phys. Lett. B **715**, 152 (2012).

[13] G. Davatz, F. Stockli, C. Anastasiou, G. Dissertori, M. Dittmar, K. Melnikov, and F. Petriello, J. High Energy Phys. 07 (2006) 037.

[14] C. Anastasiou, G. Dissertori, F. Stockli, and B. R. Webber, J. High Energy Phys. 03 (2008) 017.

[15] C. Anastasiou, G. Dissertori, M. Grazzini, F. Stockli, and B. R. Webber, J. High Energy Phys. 08 (2009) 099.

[16] S. Dittmaier, C. Mariotti, G. Passarino, R. Tanaka, S. Alekhin, J. Alwall, and E. A. Bagnaschi *et al.*, arXiv:1201.3084.

[17] T. Sjostrand, S. Mrenna, and P. Skands, J. High Energy Phys. 05 (2006) 026.

[18] G. Corcella *et al.*, arXiv:hep-ph/0210213.

[19] S. Frixione and B. R. Webber, J. High Energy Phys. 06 (2002) 029.

[20] P. Nason, J. High Energy Phys. 11 (2004) 040.

[21] A. Banfi, G. P. Salam, and G. Zanderighi, J. High Energy Phys. 06 (2012) 159.

[22] T. Becher and M. Neubert, J. High Energy Phys. 7 (2012) 108.

[23] G. Parisi and R. Petronzio, Nucl. Phys. **B154**, 427 (1979).

[24] A. Banfi, G. P. Salam, and G. Zanderighi, J. High Energy Phys. 03 (2005) 073.

[25] S. Catani, Y. L. Dokshitzer, M. H. Seymour, and B. R. Webber, Nucl. Phys. **B406**, 187 (1993).

[26] S. D. Ellis and D. E. Soper, Phys. Rev. D **48**, 3160 (1993).

[27] Y. L. Dokshitzer, G. D. Leder, S. Moretti, and B. R. Webber, J. High Energy Phys. 08 (1997) 001.

[28] M. Wobisch and T. Wengler, arXiv:hep-ph/9907280; M. Wobisch, Report No. DESY-THESIS-2000-049.

[29] M. Cacciari, G. P. Salam, and G. Soyez, J. High Energy Phys. 04 (2008) 063.

[30] F. A. Berends and W. T. Giele, Nucl. Phys. **B313**, 595 (1989).

[31] Y. L. Dokshitzer, G. Marchesini, and G. Oriani, Nucl. Phys. **B387**, 675 (1992).

[32] J. M. Campbell and E. W. N. Glover, Nucl. Phys. **B527**, 264 (1998).

[33] S. Catani and M. Grazzini, Nucl. Phys. **B570**, 287 (2000).

[34] S. Catani and M. Grazzini, Nucl. Phys. **B845**, 297 (2011).

[35] See Supplemental Material at http://link.aps.org/supplemental/10.1103/PhysRevLett.109.202001 for explicit formulas, details on the relation between jet- and boson-p_t resummations, and additional figures and references.

[36] D. de Florian, M. Grazzini, and Z. Kunszt, Phys. Rev. Lett. **82**, 5209 (1999).

[37] V. Ravindran, J. Smith, and W. L. Van Neerven, Nucl. Phys. **B634**, 247 (2002).

[38] C. J. Glosser and C. R. Schmidt, J. High Energy Phys. 12 (2002) 016.

[39] J. M. Campbell and R. K. Ellis, Phys. Rev. D **65**, 113007 (2002).

[40] J. M. Campbell, R. K. Ellis, and G. Zanderighi, J. High Energy Phys. 10 (2006) 028.

[41] J. M. Campbell, R. K. Ellis, and C. Williams, Phys. Rev. D **81**, 074023 (2010).

[42] R. Hamberg, W. L. van Neerven, and T. Matsuura, Nucl. Phys. **B359**, 343 (1991); R. Hamberg, W. L. van Neerven, and T. Matsuura, *ibid.* **B644**, 403(E) (2002).

[43] S. Dawson, Nucl. Phys. **B359**, 283 (1991).

[44] A. Djouadi, M. Spira, and P. M. Zerwas, Phys. Lett. B **264,** 440 (1991).

[45] R. V. Harlander and W. B. Kilgore, Phys. Rev. Lett. **88,** 201801 (2002).

[46] C. Anastasiou and K. Melnikov, Nucl. Phys. **B646,** 220 (2002).

[47] V. Ravindran, J. Smith, and W. L. van Neerven, Nucl. Phys. **B665,** 325 (2003).

[48] K. Melnikov and F. Petriello, Phys. Rev. Lett. **96,** 231803 (2006).

[49] S. Catani, L. Cieri, G. Ferrera, D. de Florian, and M. Grazzini, Phys. Rev. Lett. **103,** 082001 (2009).

[50] W. T. Giele, E. W. N. Glover, and D. A. Kosower, Nucl. Phys. **B403,** 633 (1993).

[51] J. M. Campbell and R. K. Ellis, Phys. Rev. D **60,** 113006 (1999).

[52] A. D. Martin, W. J. Stirling, R. S. Thorne, and G. Watt, Eur. Phys. J. C **63,** 189 (2009).

[53] M. Cacciari and G. P. Salam, Phys. Lett. B **641,** 57 (2006); M. Cacciari, G. P. Salam, and G. Soyez, arXiv:1111.6097.

[54] E. Bagnaschi, G. Degrassi, P. Slavich, and A. Vicini, J. High Energy Phys. 02 (2012) 088.

[55] S. Alioli, P. Nason, C. Oleari, and E. Re, J. High Energy Phys. 04 (2009) 002.

[56] P. Z. Skands, Phys. Rev. D **82,** 074018 (2010).

[57] S. Dittmaier *et al.* (LHC Higgs Cross Section Working Group Collaboration), arXiv:1101.0593.

[58] D. de Florian and M. Grazzini, arXiv:1206.4133.

[59] http://jetvheto.hepforge.org/.

[60] F. J. Tackmann, J. R. Walsh, and S. Zuberi, arXiv:1206.4312.